Land cover classification of rural areas using LiDAR data: a comparative study in the context of fire risk

G. Gonçalves[1,2], L. Seco[3], F. Reyes[3] & D. Miranda[3]

[1] Institute for Systems and Computers Engineering at Coimbra, Portugal
[2] Department of Mathematics, University of Coimbra, Apartado 3008, 3001-454 Coimbra, Portugal gil@mat.uc.pt
[3] University of Santiago de Compostela - Superior Polytechnical School of Lugo - Campus Universitario s/n, 27002 Lugo {lgseco,freyes,dmiranda}@usc.es

Abstract

In fire risk, correct description of topographic and fuel properties is critical to improve fire danger assessment and fire behaviour modelling. Many rural areas are now scanned using LIDAR sensors. In some of these areas the information registered by the sensor includes not only the geometric characteristics of the Earth's surface, given by the coordinates (x,y,z) of the LiDAR point cloud, but also the reflectance of the objects located on this surface, which is given by the backscattered intensity of echo reflection. The main objectives of this paper are to assess the performance of three land cover supervised classification methods of LiDAR data: Maximum Likelihood (ML), simple pixel hierarchical and object-oriented classification. In this way, three "bands" were computed from LiDAR data: the normalized height (nH), the height difference between the first and last echo (Hdiff) and the LiDAR intensity (I), which is the only spectral band of the feature space. Using data from training sites and the transformed divergence index, the separability of roads, buildings, high vegetation and low vegetation classes was evaluated. The comparison among these three classification methods was done using orthoimagery as reference data. The obtained results indicate that an evident superiority doesn't exist among the three methods.

Keywords: LiDAR, Intensity, Fire risk, Land cover, Supervised classification, Rural areas

1. Introduction

1.1 Motivation

Forest fires are one of the major challenges for natural resources management in many places in the world. Spain and Galicia are not an exception, being this autonomous community one of the most punished regions in Europe. Forest risk variables could be grouped into tree levels: topographic variables, fuel variables and variables related to human activity. Correct description of topographic and fuel properties is critical to improve fire danger assessment and fire behaviour modelling, since they guide both fire ignition and fire propagation, and fuel is the only vertex of "fire triangle" (fuel, oxygen and heat) that human action can modify directly. Moreover, in the proximity of buildings and infrastructures, there are more chances that fire was caused by higher human presence. The fact that most fires are caused by humans suggests that increased accessibility to forests will increase the possibilities of fire. Implicitly, actions around elements of special concern for humans are given priority, mainly because fire in the proximity of those places represents a risk to life. Because the safety of people and houses is a priority during fire extinction, prevention models should also consider this factor as a priority.

In this sense, correct classification of roads, buildings, high vegetation and low vegetation is very important in the later extraction of those variables. Airborne Laser Scanning (ALS), also

known as LiDAR (Light Detection And Ranging) has shown a great potential in fast and accurate geographic data acquisition below canopy closure. This active remote sensing technique records not only the geometric characteristics of the Earth's surface, but also the reflectance of the objects located on this surface. The backscattered intensity of reflection (also referred as intensity) is basically a function of the laser wavelength, which is typically in the near infrared (NIR) spectra region (0.7 - 1.5 μm for topographic applications), the range from sensor to the object and the composition and orientation of the object or surface. Because different materials have different reflectances, the intensity can be used for classifying land cover.

Nowadays, because many rural areas are scanned using Lidar sensors is indispensable to know if it is possible to use this data alone to extract the forest risk variables. Thus, the main objectives of this paper are to assess the performance of three supervised classification methods of LiDAR intensity data: maximum likelihood classification, simple hierarchical pixel classification and object-oriented classification. In this context, three bands were computed from LiDAR data: the normalized height (nH) which contain the information about the height of the objects; the height difference between the first and last echo (Hdiff); and the LiDAR intensity which is a spectral band in the NIR region. Then, using data from training sites and the transformed divergence index, the separability of the input feature space was evaluated. Finally, the object identification was made using the three classification methods. The comparison among these three classification methods was done using orthoimagery as reference data.

1.2 Related work

In spite of the great majority of the LiDAR systems have the capacity to record the received signal intensity, the great part of the published work has been done in the filtering, classification and segmentation of the 3D point cloud (x,y,z) – the primary result of LiDAR system – based on the geometric characteristics of this cloud. What is of our knowledge, a few works have been using the variable intensity in the processing of the point cloud.

Song *et al*. (2002) evaluated the possibility of using LiDAR intensity data for land-cover classification. The LiDAR point intensity has converted to a grid by using three different interpolation techniques. Using a transformed divergence method the separability of intensity data for four classes (asphalt roads, grass, house roofs and trees) has assessed. They conclude that LiDAR intensity can be used for land-cover classification and state if more features, such as DSM, and more processing, such as intensity normalization, are added better results could be reached and more classes identified.

In Matikainen *et al*. (2003) the feasibility of using LiDAR data (intensity and geometry of LiDAR point cloud) for automatic building detection in the context of map updating is investigated. Using an object-oriented classification method the feature space formed by an nDSM and by an intensity image is classified in two classes: buildings and not-buildings. A similar approach has conducted by Brennan *et al*. (2006), but considering a larger number of information classes and segmentation levels.

Charaniya *et al*. (2004) used a supervised parametric classification technique to classify roads, roofs, trees and grass. The feature space was formed by using LiDAR derived data (nDSM, intensity, height variation, difference of first and last echo) and the luminance of a grey scale aerial photo. Data fusion was made by using a classification algorithm based on the Gaussian mixture model and Expectation Maximisation. The obtained results allowed them to conclude that: i) the normalized height and height variation are important geometric features for the classification procedure; ii) the intensity and luminance (i.e. non-geometric features) are useful for separating the grass (low vegetation) from roads; iii) using the intensity as the only

non-geometric feature the overall classification was slightly worse, but the tree classification was improved. A similar work was conducted by Bartels *et al*. (2006) but adding also an 8-bit NIR aerial photo to the feature space and incorporating additional knowledge and considering contextual relationships among classes.

Finally, in Höfle *et al*. (2007) the return amplitude of each eco (that is the intensity) is corrected in order to obtain a value that is proportional or equal to the surface reflectance. The intensity variations and systematic errors due to spherical loss, topographic and atmospheric effects are corrected by two independent methods: data and model-driven approaches. They conclude that both methods can achieve a significant reduction of local intensity variation within a regular neighbour to a 1/3.5 of the original variation and offsets between flight strips to 1/10. They pointed out that the need for normalized intensity values area justified for large data sets containing strong elevation differences. As the height variations in this study are very small we used the original uncorrected intensity values.

2. Methodology

2.1 Data and study area

The study area (Figure 1) is located in the north of Galiza (Spain) and it is composed basically by a small residential zone and a forest zone, whose dominant species is Eucalyptus Globulus. In geomorphologic terms, in spite of the altitudes varying between 230 and 370m, the relief of the zone is quite accentuated.

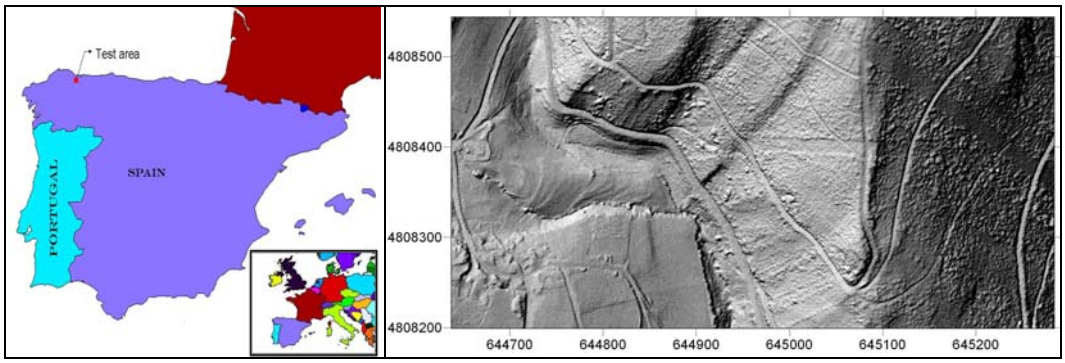

Figure 1: The location and shaded relief of the test area

The LiDAR data were acquired in November 2004 with Optech's ALTM 2033 (www.optech.ca) from a flight altitude of 1500m (ASL).The LiDAR sensor works with a laser wavelength of 1064 nm and the beam divergence was set to 0.3 mrad. The pulsing frequency was 33 kHz, the scan frequency 50 Hz, and the scan angle ±10 degrees. The first and last return pulses were registered. The complete study area was flown in 18 strips and each strip was flown three times, which gave an average measuring density of about 4 points per square meter.

2.2 Features, classes and separability

In order to run image classification methods in the LiDAR data, these (intensity and the original and the filtered point cloud) have to be converted to a grid format. Take into account the pulse density (4pts/m2) the cell size chosen was 0.5m. In this way each one of the features used in the classification procedure was derived from the original and filtered LiDAR data by using the kriging interpolation method with linear variogram. The parameters chosen for the interpolation of each grid are given in table 1. However as it was indicated in (Gonçalves, 2006) for these

sampling densities and for this cell size the influence of the interpolation method is not important for the subsequent classification procedure. The kriging interpolator was chosen by the fact that it can produce a smooth topographic surface and in the case of intensity values it can remove some of its noise more effectively.

2.2.1 Features

For image classification purposes we identify three features to be used (see figure 2):

- Normalized height (nH). This feature is obtained by subtracting the morphological filtered DTM from the original DSM. The DSM was interpolated from the first LiDAR return. The morphological adaptive filter used to obtain bare earth points from the LiDAR point cloud is described in (Gonçalves-Seco *et al*. 2007). The DTM was interpolated from these bare earth points corresponding to the last return LIDAR. This feature is created to exclude the influence of topography from the classification process and is useful to differentiate the high objects (high vegetation and buildings) from the low objects (low vegetation and roads).
- Height difference between the first and last return (Hdiff). Depending on the laser and object characteristics the LIDAR shot can penetrate through the objects and backscattered to the sensor at different height levels of the objects. In the case of first and last pulse acquisition, some of the shot energy can be returned to the sensor from the top of the penetrable objects while another part of its energy continues her path until reaching the terrain where is backscattered to the sensor. In this study this feature is used to identify the high vegetation areas, and it acts as a measure of height texture.
- Intensity (I): Since the laser unit of the LiDAR system uses light from the near infrared portion of the spectrum we use this feature to introduce spectral knowledge in the classification procedure. This is the only non-geometric information provided by the sensor and the intensity image is interpolated from the first LiDAR return.

Table 1: Kriging interpolation parameters:

Interpolated Grid	Error variance	Scale, Length, Anisotropy ratio, Anisotropy angle
DSM (first and last echo)	8.76	2,1,2,125.7
DIM	1.5	1,0,2,125.7
DTM	8.76	2,1,2,125.7

2.2.2 Classes

In the context of fires in rural areas we can devise four information classes that they play a central role in the fire risk management: roads, buildings, high vegetation and low vegetation. In fact, beyond topographic variables estimated from DTM (for example the slope, the altitude and aspect which affects, respectively, the fire spread, the occurrence and fire behaviour and regulates temperature levels and relative humidity), in the proximity of roads and buildings, there are more chances that fire was caused by higher human presence. The fact that most fires are caused by humans suggests that increased accessibility to forests will increase the possibilities of fire. Implicitly, actions around elements of special concern for humans are given priority, mainly because fire in the proximity of those places represents a risk to life. Because the safety of people and houses is a priority during fire extinction, prevention models should also consider this factor as a priority (Gonçalves-Seco *et al*., 2007b). High and low vegetation can help to represent fuel properties at surface and crown level, such as dead and live fuel load, canopy cover and height, vertical and horizontal structure of the canopy, the quantity of biomass and fuel moisture content (Pyne *et al*., 1996).

2.2.3 Separability assessment

In order to assess the signature separability in the feature space the transformed divergence method (TDI) was used. The TDI index between two classes i and j is derived from the likelihood ratio of any pair of classes and varies within in the interval [0,2] (Richards *et al.*, 2006):

$$\mathrm{TDI}_{ij} = 2 \times (1 - e^{-d_{ij}/8}) \tag{1}$$

where

- $d_{ij} = \frac{1}{2}\mathrm{T_r}\left\{(\mathbf{C}_i - \mathbf{C}_j)(\mathbf{C}_j^{-1} - \mathbf{C}_i^{-1})\right\} + \frac{1}{2}\mathrm{T_r}\left\{(\mathbf{C}_i^{-1} + \mathbf{C}_j^{-1})(\mathbf{m}_i - \mathbf{m}_j)(\mathbf{m}_i - \mathbf{m}_j)^t\right\}$
- $\mathbf{C}_i$, $\mathbf{C}_j$, $\mathbf{m}_i$, and $\mathbf{m}_j$ are the covariances and means for the classes i and j, respectively,
- $\mathrm{T_r}$ is the trace function.

The greater the value of TDI the greater is the signature separability based on this feature space and training data. In general a TDI value of 2.0 is considered to be indicator of perfect separability while a value of 0 indicates complete overlap between the signatures of the two classes. Values greater than 1.9 are considered good separability and values less than 1.7 are considered poor separability.

2.3 Classification methods

In general, image classification procedures can be categorized into supervised and unsupervised, depending on the presence of previous knowledge about the land cover types, and into parametric and nonparametric depending on the assumptions made about the multivariate normal distribution of the N-dimensional feature space. In the case of high resolution (HR) imagery data some authors (Brennan *et al*., 2006; Li *et al*., 2007) argue that is not practical to classify the image using traditional pixel-based classification methods, such as supervised parametric (e.g. maximum likelihood), because they have considerable difficulties to deal with the rich information content present in the HR 2-D data and they produce a characteristic and inconsistent salt-and-pepper classification. They purpose more advanced approaches such as object-oriented segmentation and classification techniques to overcome these problems.

In the context of land cover classification of small footprint LiDAR data (i.e high resolution 2½-D data) the maximum likelihood and object oriented methods are the more used. Because of this high spatial resolution of LiDAR data set we are interested to study also the performance of simple hierarchical classification when compared to the maximum likelihood and the more advanced object-oriented classifier.

2.3.1 Maximum Likelihood

The Maximum Likelihood Classifier (ML) is perhaps the most commonly used supervised parametric classifier because of its robustness and its easy availability in almost any image classification software package (Lu *et al*., 2007). Under the assumption of multivariate normal distribution of the classes examined a pixel **x** is classified by this method to belonging to the class w_i if it minimizes the discriminate function $g_i(\mathbf{x})$ (that is, it has the maximum likelihood of correct assignment)

$$g_i(\mathbf{x}) = (\mathbf{x} - \mathbf{m}_i)^T \mathbf{C}_i^{-1} (\mathbf{x} - \mathbf{m}_i) + \ln \mathbf{C}_i \tag{2}$$

where $\mathbf{m}_i$ and $\mathbf{C}_i$ are the mean vector and covariance matrix of the class under examination (w_i) computed from the training data.

2.3.2 Simple hierarchical classification

In this classification method we used binaries queries (or decisions) to place pixels into classes. Each query divides the pixels in a set of images into two classes based in an expression. Each new class can be divided into two more classes based on another expression. The algorithm used to build this classifier is given in figure 2 and has been implemented using *MatLab*™ language. Only three (par3,par4,par5) of the six classification parameters are computed from the intensity values of the training areas. The other three parameters are height thresholds and can be computed from the characteristic of LiDAR flight: par1 defines the minimum height of the high objects (buildings and trees); par2 defines the minimum height of penetrable objects; par6 depends on LiDAR system and defines minimum height echo separation.

Algorithm 1: Hierarchical classification

```
Input  : I[m,n] ;                                   /* Intensity image */
         nH[m,n] ;                                  /* Normalized Height image */
         Hdiff[m,n] ;                               /* Height difference image */
         Roads, Buildings, Hveg, Lveg ;             /* Attribute classes */
         par1, par2 par3, par4, par5, par6 ;        /* Classification parameters */
Output: ImClas[m,n];                                /* Classified image */
begin
    Imclas[m,n] ← 0
    foreach pixel[i,j] ∈ ImClass do
        if nH[i,j] ≥ par1 ;                         /* Separate high from low objects */
        then
            if Hdiff[i,j] ≥ par2 ;                  /* Separate penetrated objects */
            then
                pixel[i,j] ∈ Hveg
            else
                pixel[i,j] ∈ Buildings
            end
        else
            if I[i,j] ≥ par3;                       /* Maximum intensity value for roads */
            then
                pixel[i,j] ∈ Lveg
            else
                if I[i,j] ≥ par4 and I[i,j] ≤ par5; /* Intensity values for roads */
                then
                    pixel[i,j] ∈ Roads
                else
                    if Hdiff[i,j] ≤ par6;           /* Separate roads from low vegetation */
                    then
                        pixel[i,j] ∈ Roads
                    else
                        pixel[i,j] ∈ Lveg
                    end
                end
            end
        end
    end
end
```

Figure 2: Simple hierarchical classification algorithm.

2.3.3 Object-oriented classification

In object-oriented classification approaches image analysis is done in object space rather than pixel space and objects are used as the information carriers for further classification. Image segmentation is the main step that is used to convert an image into multiple objects. In *eCognition*™ software object-oriented image analysis is performed into three steps: multiresolution segmentation, creation of general classes and classification rules. In the first step,

images segments are defined and calculated using a bottom-up region-merging segmentation. In his patented algorithm (version 4.02) the parameters that control image segmentation are: scale, color, smoothness and compactness. The scale parameter (Sc) is an abstract value to determine the maximum possible change of heterogeneity caused by fusing several objects. Color (C) is the most important criteria for creating meaningful objects and defines the contribution of spectral values to define homogeneity of each object. Smoothness describes the similarity between the image object borders and a perfect square. Compactness (Cl) describes the "closeness" of pixels clustered in an object by comparing it to a circle (Baatz et all, 2004). These image segments have to be calculated on several hierarchical levels in a "trial and error" process to result in final image segments to represent single objects of interest (Navulur, K., 2006). In the second step Class Hierarchy are build by creating and defining classes. In our case, we have used only one level for the multiresolution segmentation and the parameters used for this segmentation are given in table 2. The rules used for the class definition are the same that we have used for the decision tree of the simple hierarchical pixel classification method.

Table 2: Image segmentation parameters.

Layer weights	nH = 10; I = 1; Hdiff = 1
Scale and homogeneity criterion	Sc=10; C=0.1; Cl=0.3; S = 0.7

2.4 Classification accuracy assessment

In order to assess the accuracy of the results obtained by the three classification methods a random sample of 770 points are generated and manually classified using an orthoimage of the test area. This sample is used to generate an error matrix for each classification method. From these error matrixes several measures are computed to describe the accuracy of land cover classification. As global measures we will use the overall accuracy (Pc) which gives the overall percentage of area correctly classified and the overall kappa statistic (k) which takes into account the whole confusion matrix including its off-diagonal elements. As local measures (i.e class accuracy) we will use the producer's accuracy (PA) which gives the percentage of correctly classified pixels from the collected class samples, and the user's accuracy (UA) which gives the percentage of pixels which were correctly assigned to one particular class.

3. Results

3.1 Separability of class signatures

Table 3 shows the results obtained for the separability analysis of class signatures. The average separability is 1.96 which means that the four classes forming the feature space can, in principle, be correctly separated using the signatures computed from the training data. The minimum separability is between buildings and high vegetation. This means that the feature space is not enough to achieve a good separability between these two classes.

Table 3: Separability measures using TDI. Class-1 = roads; Class-2 = buildings; Class-3 = high vegetation; Class-4 = low vegetation

Name	Class-1	Class-2	Class-3
Class-2	2.000		
Class-3	2.000	1.764	
Class-4	2.000	2.000	2.000

3.2 Classification methods

Figure 4 shows the training areas and the results of the three classification methods. Figure 4a (left) shows the training areas (in red) superimposed over the orthoimage that was used to classify manually the random sample. Note that the date of this orthoimage is previous to the date of LiDAR flight. Figure 4b, 4c and 4d shows, respectively the results obtained for the ML, simple hierarchical and object-oriented classifiers. For the simple hierarchical classifier the following values were used for the six parameters: 1.5,0.5,34,0,20,0. Although the three classifiers they produce correct and similar qualitative results, the object-oriented classifier gives visually better results in the labelling of the building and roads classes.

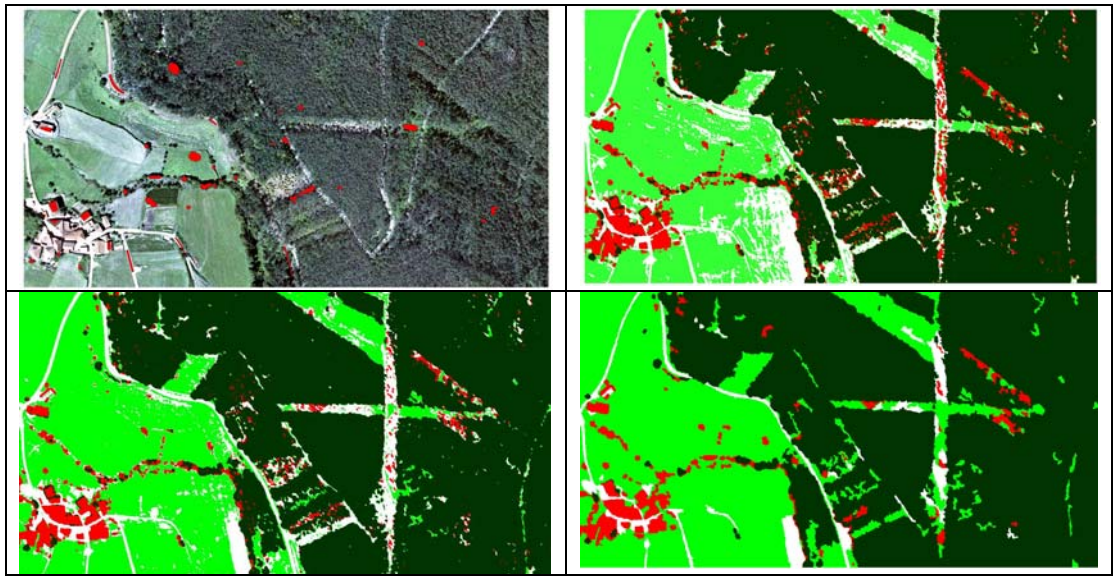

Figure 4: Training areas and results of the classification methods. First row: training data (left) and results of ML classifier (right). Second row: results of the simple hierarchical (left) and object-oriented classifiers (right)

3.3 Accuracy assessment

The error matrix and some accuracy measures for the two classification methods are given in table 4. In this table the PA and UA accuracies also given for each class. The global measures such as Pc and k are also given. The global measures indicate that the object-oriented classifier is slightly better than the ML and simple hierarchical classifiers (better Pc and K values). However the PA for the building class is higher in ML classifier than in simple hierarchical and object-oriented classifiers. In any way, for the three classifiers, the user accuracy of the roads and building classes are not good as the user accuracy of high vegetation and low vegetation.

Table 4. Error matrix and accuracy measures for the three classification methods. Legend: UA - user accuracy (%); PA - producer accuracy (%); Pc - overall accuracy; k – overall kappa statistic.

	Maximum likelihood					Simple hierarchical					Object-oriented				
	1	2	3	4	UA	1	2	3	4	UA	1	2	3	4	UA
1	20	1	00	55	26	22	6	5	50	27	18	2	0	15	51
2	1	31	22	10	48	0	28	13	4	62	0	28	11	5	64
3	0	0	414	9	98	0	0	421	10	98	0	0	424	11	97
4	4	2	7	194	94	3	0	4	204	97	7	4	8	237	93
PA	80	91	93	72		88	82	95	76		72	82	96	88	
	Pc = 85.6; K = 0.75					Pc = 87.7; K = 0.79					Pc = 91.8; K = 0.85				

4. Conclusions and future work

The obtained results indicate that it is possible to add to the traditional LiDAR point cloud classification (terrain and off-terrain points) a larger number of typical classes of these areas. The normalized height allowed the separation of the high objects from low. The LiDAR intensity allowed to unbundled the roads from the low object class and the height difference between the first and last echo allowed to isolate the objects that can be penetrated by the LiDAR shots (vegetation).

The error matrix obtained for the classification methods shows that, in the context of the forest risk of rural areas, an evident superiority doesn't exist between the three methods. In these conditions, the method of simple hierarchical pixel classification can be used in bulky LiDAR point clouds for the extraction of the four classes pertinent for the subsequent generation of the fire risk variables. However some difficulties subsist in the separation of the high vegetation and building classes. The low user accuracy verified for the roads can be due to the fact that we have put in the same class the asphalted roads and non-asphalted roads. We could think that the consideration of one more class (non-asphalted roads or forest roads) will improve the results. However, the consideration of this class would also bring the additional problem of the separation between non-asphalted roads and low-vegetation class.

The limitations of the three classifiers relates to misclassification of high vegetation and buildings, which are consistent with those of Brennan *et al*. (2006). Some others limitations/difficulties were found in the classification accuracy assessment. In fact, due to the high resolution of LiDAR data it is important that the resolution of the reference data will be much better than the LiDAR computed “images”. In case we use ortoimages as the reference data these images have to be true ortoimages, what are very difficult to achieve in forested environments. However, the use of stereoscopic images can be a solution to achieve a correct manual 3D-classification of the reference data.

Finally, as future work, we can incorporate contextual knowledge into the classifiers to distinguish between buildings and high vegetation. In fact, we intended to use the shape and area parameters to identify isolated trees in a post classification step of the simple hierarchical pixel classifier.

Acknowledgements

Many thanks to R. Crecente and R. A. Díaz Varela from the Land Laboratory of University of Santiago de Compostela for their valuables comments and suggestions. The data used in this work was funded by by the Galician Government (Xunta de Galicia) and Land Laboratory (University of Santiago de Compostela).

References

Alharthy, A., Bethel, J., 2002. “Heuristic filtering and 3D Feature extraction from LIDAR data”. *ISPRS Commission III Symposium*, Graz, Austria. September 9.

Axelsson, P., 1999. “Processing of laser scanner data – algorithms and applications”. ISPRS Journal of Photogrammetry and Remote Sensing. Vol 54, No. 2-3, Págs. 138-147.

Bartels, M., Wei, H., and Ferryman, J., 2006. Analysis of LIDAR Data Fused with Co-Registered Bands. In CD: *Proceedings of the IEEE international Conference on Video and Signal Based Surveillance* (November 22 - 24). AVSS. IEEE Computer Society, Washington, DC, 60.

Baatz, M., Benz, U., Dehghani, S., Heynen, M., Höltje, A., Hofmann, P., Lingenfelder, I., Mimler, M., Sohlbach, M., Weber, M., Willhauck, G., 2004. eCognition User Guide 4

Charaniya, A., Manduchi, R., Lodha, S., 2004. "Supervised parametric classification of aerial LIDAR data". *IEEE Conference on Computer Vision and Pattern Recognition Workshop*, Págs. 30-38.

Coren, F., Visintini, D., Prearo, G., Sterzai, P., 2005. "Integrating LiDAR intensity measures and hyperspectral data for extracting of cultural heritage". *Workshop Italy-Canada for 3D Digital Imaging and Modelling: applications of heritage, industry, medicine and land*.

Gonçalves, G., 2006. Analysis of interpolation errors in urban digital surface models created from LIDAR data. *Proceedings of 7th International Symposium on Spatial Accuracy Assessment in Natural Resources and Environmental Sciences*. pp 160-168. Lisbon, Portugal.

Gonçalves-Seco, L., Miranda, D., Crecente, R., Farto J., 2006. "Digital Terrain Model generation using airborne LIDAR in florested area of Galicia, Spain". *Proceedings of 7th International Symposium on Spatial Accuracy Assessment in Natural Resources and Environmental Sciences*. Págs. 169-180. Lisbon, Portugal

Gonçalves-Seco L., Fraga-Bugallo, B., Crecente Maseda, R., Miranda Barrós, D., 2007b. "Automatic extraction of forest and terrain fuel variables with airborne lidar to determine structural fire risk". *Proceedings of ForestSat'07*, 9 pp. Montpellier (France).

Höfle, B., Pfeifer, N., 2007. Correction of laser scanning intensity data: data and model-driven approaches. *ISPRS Journal of Photogrammetry and Remote Sensing*, 62 415-433.

Li, H., Gu, H., Han, Y. and Yang, J., 2007. Fusion of High-Resolution Aerial Imagery and LIDAR Data for Object-oriented Urban Land-cover Classification Based on SVM. *ISPRS Workshop on Updating Geo-spatial Databases with Imagery & The 5th ISPRS Workshop on DMGISs*, Urumchi, China. http://www.commission4.isprs.org/urumchi/ (accessed 7 March 2008)

Lu, D. and Weng, Q., 2007. A survey of image classification methods and techniques for improving classification performance. *International Journal of Remote Sensing*, 28:5, 823 - 870

Maas, H.-G., 1999. "The potential of height texture measures for the segmentation of airborne laserscanner data". *Fourth International Airborne Remote Sensing Conference and Exhibition / 21st Canadian Symposium on Remote Sensing*, Ottawa, Ontario, Canada, 21-24 June.

Matikainen, L., Hyyppä, J., Hyyppä, H., 2003. Automatic detection of buildings from laser scanner data for map updating. *International Archives of Photogrammetry, Remote Sensing and Spatial Information Sciences* 34 (Part 3/W13), 218–224.

Navulur, K., 2006. Multi-spectral image analysis using the object oriented paradigm. CRC Press, Inc.

Pyne, S. J., Andrews, P. L., & Laven, P. D., 1996. Introduction to wildland fire. New York: Wiley & Sons Press: 22–45.

Richards, J. A. and Jia, X., 2006. Remote Sensing Digital Image Analysis: an Introduction. 4rd. Springer-Verlag New York, Inc.

Sithole, G., 2005. "Segmentation and classification of Airborne Laser Scanner Data". Publications on Geodesy 59. Nederlandse Commissie voor Geodesie, Delft, The Netherlands, 184 pgs.

Song, J.H., Han, S.H., Yu, K.Y., Kim, Y.I., 2002: "Assessing the possibility of land-cover classification using LIDAR intensity data". *ISPRS Commission III Symposium*, Graz, Austria. September 9.